INFLUENCE OF SURFACE INTEGRITY BY PRECISION HARD TURNING ON ROLLING CONTACT FATIGUE

N. JOUINI[a] , P. REVEL[a*], G. THOQUENNE[b], M. BIGERELLE[a,c]

a Laboratoire Roberval, UMR 6253, UTC/CNRS, Centre de Recherche de Royallieu, 60205 Compiègne, France.
b Centre Technique des Industries Mécaniques (CETIM), 52 avenue Felix Louat, 60300 Senlis, France
c Laboratoire Thermique, Energétique, Mise en forme, Production, EA 4542, Université de Valenciennes et du Hainaut Cambrésis, Le Mont Houy, 59313 – Valenciennes, France.

*Corresponding Author: philippe.revel@utc.fr

Abstract: Traditionally, components of hardened steels, such as bearings, gears, shafts, and rails are finished by grinding process. Precision hard turning has become a competitive finishing process with respect to grinding process. In this paper, the relationship between surface integrity and fatigue life of AISI 52100 bearing steel (60-62 HRC), is investigated. Machining experiments are carried out varying cutting parameters under dry condition using cubic Boron Nitride (c-BN) cutting tools. Fatigue life tests are performed on a twin-disk machine. The surface integrity is characterized by surface roughness measurements, subsurface microstructure observations and residual stresses evaluation. The SEM observations of the transversal cross-section show the presence of very fine white layer (<1µm) on the top surface and thermal affected zone of 35 µm in the sub-surface. Experimental results suggest that the effect of surface roughness on RCF life is more significant than the effect of the level of compressive residual stresses. Indeed, RCF life decreases with the increase of the average roughness (R_a). The roller bearing components can attain 5.2 million cycles with R_a = 0.11 µm, and 0.32 million cycles with R_a = 0.25 µm. In comparison with grinding processes, the bearing components attaint 1.2 million cycles with conventional grinding (R_a = 0.2 µm) and 3.2 million cycles with grinding followed honing (R_a = 0.05 µm). Therefore, the high precision hard turning allows improving the surface integrity and RCF life of the roller bearing components.

1 INTRODUCTION

Bearing steel components are widely used in heavy mechanical industry e.g. aerospace, automotive, etc. These components are subjected to severe operating conditions such as high loads, high speed, extreme temperatures and hostile environments. Thus, bearing steel such as AISI 52100 is thermally treated to achieve martensitic structure that enhances desired mechanical properties, fatigue strength and wear resistance. Then, it is finished in its hardened state by grinding process to achieve surface integrity. However, precision hard turning, defined as single point cutting of part with hardness of material in excess of 45 HRC under small feed rate and fine depth of cut conditions, has become an attractive alternative to grinding process [1]. It offers very substantial benefits with respect to grinding process such as environment-friendly, low surface roughness amplitude [2], capability to generate complex workpiece geometry and induces deep compressive residual stresses that often increase the fatigue life [3]. In literature, the rolling contact fatigue (RCF) life of bearing steel components is heavily influenced by the surface topography [4,5] as well as metallurgical and mechanical state of the subsurface layers [6].

The fatigue life of bearings is determined by the detachment of material (spalling) following the initiation of cracks below the contact surface, spalling due to surface irregularities and due to the distress caused by surface roughness or inadequate lubrication [7,8,9]. In the case of hardened steel, fatigue origins have resulted in a preponderance of surface asperities [10,11]. Thus, roughness is considered as one of the main causes of crack initiation for hard steel components.

However, hard turning can introduce modifications within the surface layer of a workpiece. These modifications are metallurgical transformations as result of intense, localized and rapid thermo-mechanical loading. The surface layer can show an extremely different structure from the bulk material due to the white layer formation that appears white in colour under an optical microscope after polishing and etching or featureless in a scanning electron microscope [12]. It is referred to as untempered martensite [13] and characterized by an increased in hardness than the bulk material [12,13,14]. The mechanism of white layer formation is attributed to severe plastic deformation, which produces a homogenous structure or one with a very fine grain size, and/or rapid heating and quenching, which results in phase transformation [13,15].

The white layer induced by hard turning was detrimental to component fatigue life [2,16]. Indeed, the thicker the white layer, the shorter the RCF life [11]. However, despite white layer occurrence, hard turning provides greater fatigue life than grinding process [17,18]. This can be explained by the compressive residual stresses induced by hard turning.

In this study, at the beginning an experimental design was carried out by machining 8 samples; this experimental design was then supplemented by an additional test. Later, microstructure analyses were carried out and the effects of surface roughness amplitude, characterized by the R_a value, and of residual stresses level, measured by

X Ray diffraction, on rolling contact fatigue life were studied. Finally, a comparative analysis between precision hard turning, grinding, and grinding followed by honing was performed.

2 EXPERIMENTAL WORK

2.1 Experimental set-up and machining tool

The machining tests were conducted on high precision turning machine, as shown in figure 1. This machine is a prototype lathe, designed by SnecmaTM Motor with a T-slide architecture and now presents in the Roberval laboratory, where it was improved, notably in the field of control [19,20]. The two slides-ways (X- and Z-axis) are guided by hydrostatic-bearings offering low friction, high stiffness and high damping; fixed on a massive granite block (1.5 tonne), itself resting on four self-levelling pneumatic isolators. The straightness of both slides is better than 0.3 µm for a displacement of 100 mm. The spindle is mounted axially to the Z-axis and an active magnetic bearing is adopted to achieve greater spindle dynamic stiffness. Due to the high accuracy needed along X- and Z-axis, ironless linear motors ILD 24-050 (ETELTM) are used for feed drive system. Each linear axis is operated by a position control system controlled using an incremental linear encoders LIP 401R (HeindenhainTM) having 4 nm resolution. Displacements are controlled by a computer numerical control system with a powerful numerical card (Programmable Multi-Axis Controller: PMAC-DeltatauTM).

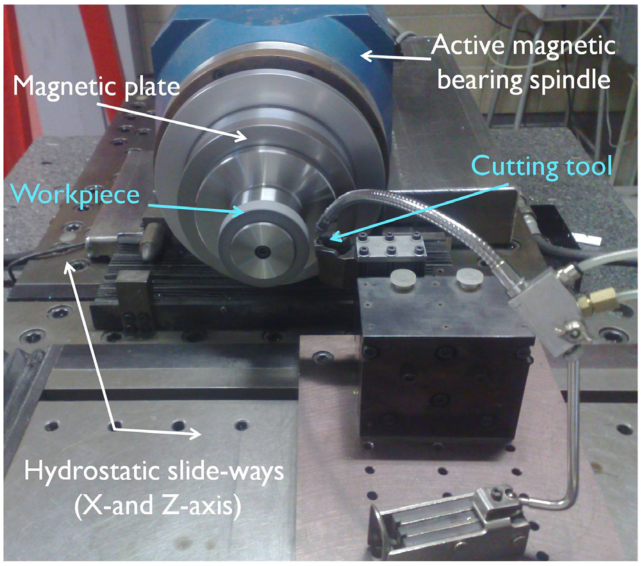

Figure 1: Focus on the high precision turning machine used in this study.

The machining tests were performed under dry cutting conditions using c-BN cutting tool inserts (ISO code CNGA 120408 S01030 7025) manufactured by SandvikTM Coromant. The inserts were mounted using a Coro torn RC rigid clamp system in the tool holder DCLN 2525M12 (ISO), providing the following angles: rake angle $\gamma 0$= -6°, inclination angle λs= -6°, cutting edge angle χr= 95°, clearance angle α= 6° and nose radius r= 0.8 mm.
In this work, AISI 52100 bearing steel rings thermally treated to an average hardness of 61±1 HRC were used as workpiece material. The length of the ring was 14 mm with outer diameter of 70 mm and the inner diameter of 19 mm.
A full factorial experimental design (2^3) was performed to analyse the effect of cutting parameters (cutting speed, feed rate and depth of cut). Table 1 shows the full set of the eight experiments.

Table 1: Experimental design matrix

Experiments n°	Depth of cut ap (µm)	Cutting speed Vc (m/min)	Feed rate f (µm/rev.)
1	5	210	50
2	5	210	100
3	5	260	50
4	5	260	100
5	10	210	50
6	10	210	100
7	10	260	50
8	10	260	100

An additional test (n°9) was performed with the following conditions: ap=5 µm; Vc=360 m/min; f =50 µm/rev.

2.2 Surface roughness measurement

The measurements were carried out by stylus profiler 3D KLA-TencorTM (P-10 model) with a 2 µm tip radius, loaded with 50 mN [21]. For each specimen, 25 roughness profiles were recorded perpendicular to the grooves. The scanning length and the sampling length were respectively 8 mm and 0.1 µm (80 000 data points along the profile length). Each profile was rectified by a third degree polynomial fit to remove the form of the surface. Then, the surface roughness amplitude (R_a) was computed.

2.3 Microstructure analyses

The cross-section of each sample was prepared for microscopic analysis using traditional metallographic techniques. The samples were carefully sectioned with an abrasive cutter, mounted in a thermosetting resin with carbon filler (PolyFast) for SEM examination, followed by gentle grinding and polishing with diamonds, successively using grain sizes of 6, 3 and 1 micron, then etched using a 2% Nital solution for approximately 10 s. The micrographic analyses of cross-sections were then carried out using scanning electron microscope (Philips XL30 ESEM-FEG).

2.4 X ray analyses

In order to have diffraction, it is necessary that the law of Bragg is satisfied. The X-Ray diffraction analyses have been carried out by using Cr-Kα radiation diffracted at $2\theta = 156°$ in the atomic plan (211) of steel. These conditions give the strain localised at a depth of 6 µm (according to EN-15305 standard: Test methods for residual stress analysis by X-ray diffraction). The analyses are realised in the radial and longitudinal directions, in four locations. The X-Ray spot size is adapted to the measurement zone. For each direction ϕ, 7 angles of incidence ψ *(*$\psi=0$ *et* $6\psi>0$*)*, are considered to obtain equivalent interval in the $\sin^2\psi$ axe and to have $0 \leq \sin^2\psi \leq 0{,}45$.

The diffraction pattern position is determined by the centred barycentre method developed by CETIM and recognised in the standard. The radiocristallographic constants used for the reflexion plan (211) in the residual stress calculation are: $\frac{1}{2} S_2 = 5{,}83\ 10^{-6}\ MPa^{-1}$ $S_1 = -1{,}28\ 10^{-6}\ MPa^{-1}$

In order to make a quantitative analyse of the structural phases in the material, an analyse of the diffraction by energy dispersion was performed. If a value of θ, identified before as correspondent with a peak of the diffraction diagram, only photons X having corresponding energy E are diffracted. The examination of the spectrum of energy by adjusting the experimental diagram thanks to an ideal model is a fast solution, which was adopted and developed by CETIM. Volumes of the phases as austenite are calculated starting from the parameters of adjustment. The precision to the measure in the standard cases is lower than one percent; this technique makes it possible to precisely evaluate the percentages of carbides present and the martensitic phase, like its percentage of carbon.

2.5 Rolling contact fatigue test rig

RCF tests are performed on a twin-disc test rig (figure 2), specifically designed by CETIM to investigate the contact between gear teeth or ring and rolling elements. The two discs rolled under pure rolling conditions and lubricated by oil injection (Mobil Gear 629, kinematic viscosity of 15.8 cSt at 100°C). The normal load is applied by a pneumatic cylinder. In the test rig, the lower disc is cylindrical (machined disc), while the upper disc is crowned (figure 3). The geometry of the contact surfaces provides an elliptical contact area for applied load 1100 daN which corresponds to a Hertzian pressure of 3.8 GPa.

Two proximity Hall-effect sensors are used to detect initiate spalling on the surfaces. The test is stopped when one of the sensors detects a spalling or reach 10 million cycles.

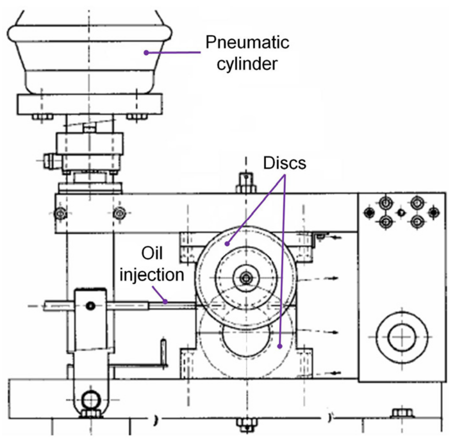

Figure 2: Schematic view of twin-disc test rig.

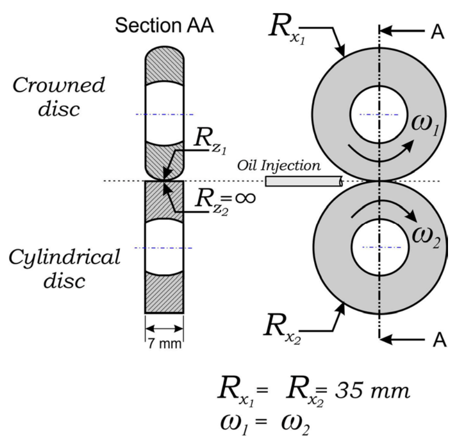

Figure 3: Geometry of RCF test sample.

3 ANALYSES AND MEASUREMENTS OF MACHINED SAMPLES

3.1 Microstructure of surface and sub-surface layers

The Scanning Electron Microscopy (SEM) observations of the cross-section of each specimen clearly revealed metallurgical transformations in the subsurface. This can be seen as an affected layer which consists of a fine white layer on the top surface, followed by an optical transition zone and then the bulk material. Whatever the samples, the observations are similar and that selected in figure 4 is quite representative.

The thickness of the white layer was evaluated below 1 µm and is statistically constant with a mean value of 0.7 µm. According to literature [12,22], the thickness of the white layer obtained during hard turning of AISI52100 bearing steel should be between 3 and 50 µm. The low depth of cut (5 µm) can explain the median value of 0.7 µm found in this study.

Under the white layer, the thickness of the transition zone is optically estimated about 40-50 µm. It should be noted that this thickness is homogenous for all the specimens (statically tested by analysis of variance).

These results show that precision hard turning generates both homogeneous thicknesses of the white layer and the transition zone. Thus, homogeneous microstructure is obtained whatever the cutting parameters under investigation.

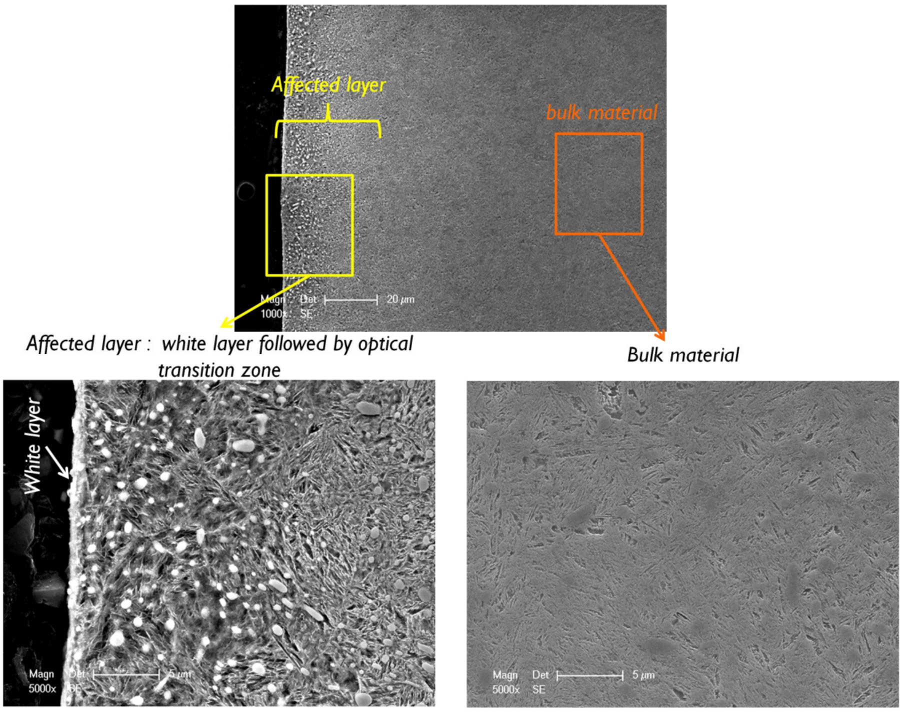

Figure 4: Subsurface microstructure relative to sample 4.

3.2 Surface roughness

According to a previous study [23], using an expert system [24,25], the roughness amplitude Ra is considered as relevant roughness parameter to characterise the surface roughness obtained by precision hard turning with different cutting parameters. The R_a values of the nine investigated specimens are summarized in table 2. Under fine depth of cut of 5 µm, the results show that the feed rate affects the R_a value. It has an increasing effect (from R_a= 0.1 µm for sample 1 to R_a= 0.25 µm for sample 2) for a cutting speed of 210 m/min. Indeed, it is well known that the theoretical value of the roughness amplitude R_a is primarily a function of feed rate for a given nose radius. Moreover, the optimal roughness amplitude R_a was obtained at cutting speed of 210 m/min (sample 1), which was considered as high cutting speed in finish hard turning of AISI 52100, and also a very high cutting speed of 360 m/min (sample 4).

3.3 X ray measurements

Residual stress measurements, in the cut direction or in feed direction are always in compression (table 2). Generally their levels are higher in feed direction than in the cut direction. The compressive stresses on the surface are an advantage for the resistance to rolling contact fatigue since that delays the crack initiation. It should be noted that in the case of ground surfaces, residual stresses are either in traction or in low compression.

The level of the residual stresses of compression is not function of level of roughness. On the other hand, it is interesting to note that more the cutting speed is high, more the level of the compression stresses in absolute value is high (tests 4,7,8,9).

The results in DXDE show that high precision machining does not modify in important proportion the phases in material, since the proportion of martensite in the bulk material is about 95% and the carbide phase is about 5%.

The fact that the residual austenite rate remains very low is a very positive point, because a good resistance to fatigue contact required a rate lower than 5%.

Table 2: Results of measurements on machined surface of roughness, residual stresses and percentage of phases[1].

Experiments n°	R_a (µm)	Residual stresses (feed direction) (MPa)	Residual stresses (cut direction) (MPa)	Martensite (%)	Carbides (%)	Residual austenite (%)
1	0.11	-248	-512			
2	0.25	-547	-356			
3	0.14	-437	-120	91.5	8.2	0.3
4	0.14	-812	-344	91.0	8.6	0.4
5	0.17					
6	0.45					
7	0.19	-1051	-396	92.9	6.9	0.2
8	0.17					
9	0.11	-1058	-270	88.3	10.7	1.0

4 ROLLING CONTACT FATIGUE TESTS

4.1 Effect of surface roughness on rolling contact fatigue life

The results of rolling contact fatigue life, by taking as reference the number of stress cycles required to reach spalling of test samples, are reported in table 3. The results show that RCF life increases as Ra value decreases. Indeed, with a higher level of roughness amplitude (R_a= 0.25 µm), the RCF life reaches 0.32 million cycles, whereas with a very low level of roughness amplitude (R_a= 0.11 µm), the RCF life reaches 3.2, even 5.2 million cycles. Therefore, high level of roughness amplitude R_a has a very detrimental effect on RCF life.

Table 3: Rolling contact fatigue cycles before failure.

Experiments n°	Ra (µm)	Number of cycles
1	0.11	5.20E6
2	0.25	0.32E6
3	0.14	2.82E6
4	0.14	3.70E6
7	0.19	1.09E6
9	0.11	3.24E6

4.2 Evolution of residual stresses and phases after rolling contact fatigue tests

The results of rolling contact fatigue life do not show a relation with the initial level of the residual stresses: a higher fatigue life do not correspond necessarily to samples with high level compression stresses.
Otherwise, the residual stress measurements after the fatigue contact tests show in the table 4, that the level of stresses decreases in absolute value, and this more especially as their starting level was high in absolute value. Moreover, at the end of the lifetime (RCF) the residual stresses measured on the surface remain in compression and on an almost identical level.
In addition, the percentage of phases measured on the surface does not change following the fatigue contact tests.

Table 4: Results of measurements on machined surfaces after rolling fatigue of residual stresses and percentage of phases.

Experiments n°	Residual stresses (feed direction) (MPa)	Residual stresses (cut direction) (MPa)	Martensite (%)	Carbides (%)	Residual austenite (%)
3	-321	-343	91.5	8.0	0.5
4	-246	-197	90.8	8.7	0.5
7	-265	-313	91.7	7.9	0.4
9	-532	-133	87.7	11.1	1.2

[1] all the samples were not analyzed by X Ray diffraction or DXDE.

4.3 Life comparison of precision hard turned vs. ground, and ground followed by honed specimens

In order to evaluate the impact of the precision hard turning process on rolling contact fatigue life of bearing steel components, a quantitative comparison between precision hard turning, grinding, and grinding followed by honing has been performed. The RCF life tests of ground sample and ground followed by honed sample were performed under the same conditions of precision hard turned samples. Figure 5 indicates that the sample achieved 1.2 million cycles with conventional grinding (R_a= 0.2 µm) and 3.2 million cycles with grinding followed honing (R_a= 0.05 µm). Thus, precision hard turning, which reaches 3.2 or 5.2 million cycles with surface roughness amplitude R_a= 0.11 µm, offers (approximately 200 to 350%) longer RCF life than grinding process and is equivalent even better than grinding followed by honing. Whereas, the roughness amplitude (R_a= 0.05 µm) obtained with grinding followed by honing is lower, precision hard turning offers an equivalent RCF life, which may induce better surface integrity. Therefore, the precision hard turning allows us to improve the surface integrity and RCF life of the roller bearing components.

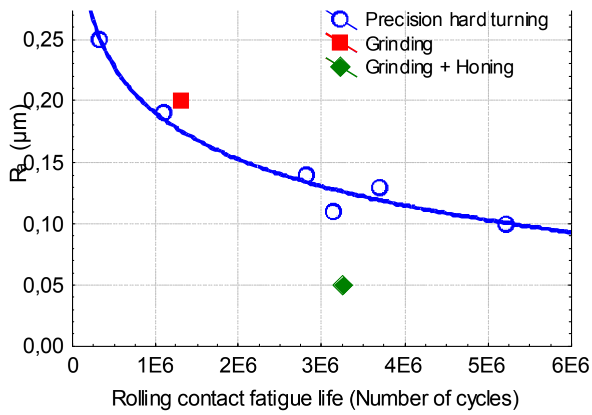

Figure 5: Life comparison of precision hard turned vs. ground, and ground followed by honed specimens.

5 CONCLUSION

This paper investigate the feasibility of the precision hard turning as finishing process to improving the rolling fatigue life of the bearing steel components.
The results can be summarized as follows:

- Precision hard turning generates homogeneous thicknesses of fine white layer and transition zone.
- RCF life of bearing steel components machined by precision hard turning reached 5.2 million cycles (at R_a= 0.11 µm) and 0.32 million cycles (at R_a= 0.25 µm). Therefore, RCF life increases as the roughness amplitude R_a decreases.
- On the other hand, RCF life is not in relation with the level of compression residual stresses, due to the high precision process.
- In comparison with precision hard turning (RCF life reaches 5.2 million cycles for R_a= 0.1 µm), the RCF life of the bearing components finished by grinding process reached 1.2 million cycles (R_a= 0.2 µm), whereas in grinding followed by honing process reached 3.2 million cycles (R_a= 0.05 µm).

Future investigations by X Ray diffraction and DXDE will be made in-depth to measure the thickness of the layer in compression and its evolution after fatigue contact tests. Moreover, analyses by grazing incidence X ray diffraction technique could give interesting information on the depth of the layer, which is modified by high precision machining [26].

6 REFERENCES

[1] König W., Berktold A., Koch K.F., *CIRP Annals - Manufacturing Technology*, 42, 1993, 39-43.
[2] Klocke F., Brinksmeier E., Weinert K., *CIRP Annals - Manufacturing Technology*, 54, 2005, 22-45.
[3] Matsumoto Y., Hashimoto F., Lahoti G., *CIRP Annals - Manufacturing Technology,* 48, 1999, 59-62.
[4] Novovic D., Dewes R.C., Aspinwall D.K., Voice W., Bowen P., *International Journal of Machine Tools and Manufacture*, 44, 2004, 125-134.
[5] Paulin C., Ville F., Sainsot P., Coulon S., Lubrecht T., the 30th Leeds-Lyon Symposium on Tribology, Elsevier Tribology and Interface Engineering Series, vol 43, 2003, 611-617.

[6] Field M, Kahles JF., The Surface Integrity of Machined and Ground High Strength Steels, DMIC Report 1964, 210, 54-77.
[7] Bhadeshia H.K.D.H., Progress in Materials Science, 2012, 57, 268-435.
[8] Olver A.V., Proceedings of the Institution of Mechanical Engineers, Part J: Journal of Engineering Tribology 2005, 219, 313-330.
[9] Liu J.Y., Tallian T.E., McCool J.I., *Tribolgy Transaction*, 1975, 18, 144-52.
[10] Tallian T.E., Failure atlas for hertz contact machine elements, ASME Press, New York, 1992,
[11] Schwach D.W., Guo Y.B., *International Journal of Fatigue,* 2006, 28, 1838-1844.
[12] Tonshoff H., Arendt C., Ben Amor R., *CIRP Annals - Manufacturing Technology,* 2000, 49, 547-566.
[13] Griffiths B.J., *Journal of Tribology-Transactions of the ASME*, 1987, 109, 525-530.
[14] Akcan S., Shah S., Moylan S.P., Chhabra P.N., Chandraseksar S., Yang H.T.Y., *Metallurgical and Materials Transactions A,* 2002, 33, 1245-1254.
[15] Ramesh A., Melkote S.N., Allard L., Riester L., Watkins T.R., *Materials Science and Engineering A*, 2005, 390, 88-97.
[16] Smith S., Melkote S.N., Lara-curzio E., Watkins T.R., Allard L., Riester L., *Materials Science and Engineering A*, 2007, 459, 337-346.
[17] Abrao A.M., Aspinwall D.K., *Wear*, 1996, 196, 279-284.
[18] König W., Klinger M., Link R., *CIRP Annals - Manufacturing Technology* , 1990, 39, 61-64.
[19] Gautier A., Khanfir H., Revel P., Fillit R., *International Journal of Machining and Machinability of Materials*, Vol. 4, N°2/3, 2008, 133-147.
[20] Khanfir H., Bonis M., Revel P., *International Journal of Machine Tools and Manufacture*, 45, 7-8, 2005, 841-848.
[21] Jouini N., Gautier A., Revel P., Mazeran P.E., Bigerelle M., *International Journal of Surface Science and Engineering*, Vol. 3, N°4, 2009, 310-327.
[22] Chou Y.K., Evans C.J., *International Journal of Machine Tools and Manufacturing*, 1999, 39, 1863-1881.
[23] Jouini N., Revel P., Bigerelle M., Proceedings of 4th CIRP International Conference on High Performance Cutting, vol 1, 2010, 23-32.
[24] Bigerelle M., Gautier A., Iost A., *Sensors and Actuators B: Chemical,* 2007, 126, 126-137.
[25] Najjar D., Bigerelle M., Iost A., *Wear,* 2003, 254, 450-460.
[26] Revel P., Khanfir H., Fillit R., *Journal of Materials Processing Technology*. 178, 1-3, 2006, 154-161